

# Multinuclear Magnetic Resonance and Mutagenesis Studies of the Histidine Residues of Human Mitochondrial Ferredoxin<sup>†</sup>

Bin Xia,<sup>‡,§</sup> Hong Cheng,<sup>§,||</sup> Lars Skjeldal,<sup>§,⊥</sup> Vincent M. Coghlan,<sup>#,∇</sup> Larry E. Vickery,<sup>#</sup> and John L. Markley<sup>\*,‡,§</sup>

Graduate Biophysics Program and Department of Biochemistry, College of Agricultural and Life Sciences, University of Wisconsin—Madison, 420 Henry Mall, Madison, Wisconsin 53706, and Department of Physiology and Biophysics, University of California, Irvine, California 92717

Received July 22, 1994; Revised Manuscript Received October 7, 1994<sup>®</sup>

**ABSTRACT:** Human mitochondrial ferredoxin is a [2Fe–2S] protein that functions to transfer electrons from NADPH-dependent ferredoxin reductase to cytochrome P450 enzymes. Two of the three histidines of human ferredoxin are strictly conserved in the sequences of all known vertebrate ferredoxins, and one of these (His<sup>56</sup>) is adjacent to Cys<sup>55</sup>, which serves as one of the ligands to the iron–sulfur cluster. All but 16 of its residues show sequence identity with those of bovine ferredoxin. It has been proposed for bovine ferredoxin that His<sup>56</sup> hydrogen bonds with a labile sulfur and that the reduction of the iron–sulfur center is accompanied by the uptake of a proton by this histidine [Lambeth, J. D., Seybert, D. W., Lancaster, J. R., Jr., Salerno, J. C., & Kamin, H. (1982) *Mol. Cell. Biochem.* 45, 13–31]. In this paper, we report procedures for labeling human ferredoxin uniformly with <sup>15</sup>N using <sup>15</sup>NH<sub>4</sub>Cl and selectively with <sup>13</sup>C by the incorporation of [U-<sup>13</sup>C]histidine. Most of the imidazole <sup>1</sup>H, <sup>13</sup>C, and <sup>15</sup>N resonances of the three histidines have been assigned by heteronuclear two-dimensional single- and multiple-bond correlation spectroscopy. Site-directed mutagenesis was used in assigning the NMR signals from His<sup>56</sup>. The pK<sub>a</sub> values of His<sup>10</sup> (6.5) and His<sup>62</sup> (5.8) in oxidized human ferredoxin were found to be similar to those reported previously for the corresponding residues of bovine ferredoxin [Greenfield, N. J., Wu, X., & Jordan, F. (1989) *Biochim. Biophys. Acta* 995, 246–254; Miura, S., Tamita, S., & Ichikawa, Y. (1991) *J. Biol. Chem.* 266, 19212–19216]. The pK<sub>a</sub> value for His<sup>56</sup> was found to be abnormal; the residue does not titrate between pH 6.0 and 8.6 in either the oxidized or the reduced state, and analysis of the <sup>15</sup>N chemical shift indicates that its pK<sub>a</sub> value is <5. pH dependence (pH<sub>mid</sub> ~7.2) was observed for the reduction potential of the iron–sulfur cluster in this class of ferredoxins [Cooper, D. Y., Schleyer, H., Levin, S. S., & Rosenthal, O. (1973) *Ann. N.Y. Acad. Sci.* 212, 227–247]; the results show that such a pH dependence, if present in human ferredoxin, would not involve histidine residues, as proposed for bovine ferredoxin. The lack of a strong temperature dependence for the <sup>1</sup>H NMR chemical shifts of any of the histidines rules out a direct interaction between any of these residues and the iron–sulfur cluster.

Vertebrate ferredoxins are small (13–14 kDa) acidic proteins with a single [2Fe–2S] cluster that are found in the mitochondria of steroid-metabolizing tissues. They function to transfer reducing equivalents from NADPH-dependent ferredoxin oxidoreductase to cytochrome P450<sub>sc</sub><sup>1</sup> enzymes involved in the biogenesis of steroid hormones, the formation of vitamin D metabolites, and the production of bile acids. Human mitochondrial ferredoxin has been found

to be involved in the initial step of progesterone biosynthesis, in which the side chain of cholesterol is cleaved to yield pregnenolone (Mason et al., 1971; Simpson et al., 1978).

The amino acid sequences of all six known vertebrate-type ferredoxins, from human placenta (Mittal et al., 1988), cow (Okamura et al., 1985), pig (Tanaka et al., 1973), chick (Kagimoto et al., 1988), sheep (Matsuo et al., 1992), and rat (Mellon et al., 1991), exhibit a high degree of sequence identity (Figure 1). The four cysteines that ligate the iron

<sup>†</sup> Presented at the NATO Advanced Research Workshop on Nuclear Magnetic Resonance of Paramagnetic Macromolecules (Chae et al., 1994). This research was supported by Grant DK30109 from the National Institutes of Health (to L.E.V.), U.S. Department of Agriculture Grant 92-37306-2699, and National Science Foundation Grant MCB-9215142 (to J.L.M.). Spectroscopy was performed at the National Magnetic Resonance Facility at Madison, WI, and supported by National Institutes of Health Grant RR02301 from the Biomedical Research Technology Program, Division of Research Resources, and the University of Wisconsin. Additional funds for equipment came from the NSF Biological Biomedical Research Technology Program (DMB-8415048), NIH Shared Instrumentation Program (RR02781), and the U.S. Department of Agriculture. L.S. was supported by a grant from the Norwegian Research Council for Science and Humanities (NAVF).

\* Author to whom correspondence should be addressed.

<sup>‡</sup> Graduate Biophysics Program, University of Wisconsin—Madison.

<sup>§</sup> Department of Biochemistry, University of Wisconsin—Madison.

<sup>||</sup> Present address: Mayo Clinic and Research Foundation, Department of Pharmacology, Guggenheim 7, Rochester, MN 55905.

<sup>⊥</sup> Present address: Department of Biochemical Sciences, Agricultural University of Norway, IBF, Kjemi boks 5036, N-1432 Ås, Norway.

<sup>#</sup> University of California—Irvine.

<sup>∇</sup> Present address: Vollum Institute, Oregon Health Sciences University, Portland, OR 97201.

<sup>®</sup> Abstract published in *Advance ACS Abstracts*, November 15, 1994.

<sup>1</sup> Abbreviations: 1D, one-dimensional; 2D, two-dimensional, COSY, homonuclear correlated spectroscopy; DEP, diethyl pyrocarbonate; DQF, double-quantum-filtered; DTT, dithiothreitol; DSS, sodium 2,2-dimethyl-2-silapentane-5-sulfonate; *E. coli*, *Escherichia coli*; HMBC, heteronuclear multiple-bond correlated spectroscopy; HSMQC, heteronuclear single and multiple quantum correlated spectroscopy; IPTG, isopropyl thiogalactoside; LB medium, Luria–Bertani medium; NMR, nuclear magnetic resonance; OD<sub>600</sub>, optical density at a wavelength of 600 nm; pH\*, pH value of a <sup>2</sup>H<sub>2</sub>O-containing solution measured with a combination glass electrode calibrated with normal H<sub>2</sub>O buffers and reported without correction; ppm, parts per million; scs, side-chain cleavage.

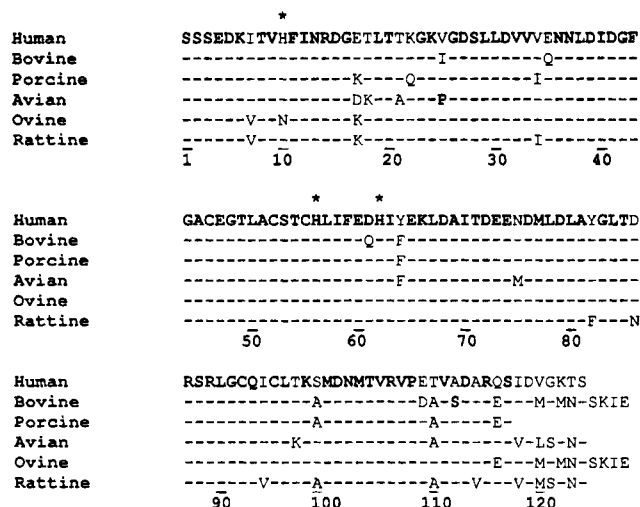


FIGURE 1: Amino acid sequences of six vertebrate mitochondrial ferredoxins: human ferredoxin (Mittal et al., 1988), bovine ferredoxin (Okamura et al., 1985), porcine ferredoxin (Tanaka et al., 1973), avian ferredoxin (Kagimoto et al., 1988), ovine ferredoxin (Matsuo et al., 1992), and rattine ferredoxin (Mellon et al., 1991). The rat ferredoxin sequence is a partial sequence. Residues conserved in all ferredoxins are indicated in boldface type. The positions of the histidine residues of human ferredoxin are shown by asterisks.

atoms of the cluster are strictly conserved at residue positions 46, 52, 55, and 92. A fifth cysteine, conserved at position 95, has been shown not to be a cluster ligand or otherwise required for activity (Cupp & Vickery, 1988). Histidines at positions 10, 56, and 62 in the sequences of human, bovine, porcine, avian, and rattine ferredoxins are conserved; ovine ferredoxin has an asparagine instead of a histidine at position 10, but contains the other two conserved histidines. One of the conserved histidines (His<sup>56</sup>) is immediately adjacent to one of the cysteines that ligates the [2Fe-2S] cluster (Cys<sup>55</sup>). A histidine at this position appears to be a feature that distinguishes these ferredoxins from plant-type [2Fe-2S] ferredoxins, which have an alanine at this position.

Conserved aromatic residues near the iron-sulfur cluster are of interest as candidates for possible roles in electron transfer. For example, recent results from mutagenesis and electron transfer studies have shown that an aromatic residue at position 65 in *Anabaena* 7120 vegetative ferredoxin is essential for rapid electron transfer (Hurley et al., 1993). In addition, a histidine residue has been implicated as a modulator of the activity of a ferredoxin: experimental evidence indicates that the electrostatic interaction between a histidine side chain and an iron-sulfur cluster is responsible for the pH dependence of reduction potential in the ferredoxin from *Clostridium thermosaccharolyticum* (Smith et al., 1991).

The reduction potential of bovine ferredoxin (-291 mV at pH 7.5) is pH dependent with a  $pH_{mid}$  of 7.2 (Cooper et al., 1973). A  $pK_a$  of 7.2 was also found in pH titration studies of the UV-visible spectrum of bovine ferredoxin (Lambeth & Kamin, 1979). The midpoint of this titration is in the range expected for the  $pK_a$  of the imidazole side chain of a histidine. Spinach ferredoxin, which does not have a histidine residue near the iron-sulfur cluster, has a much more negative and pH-independent reduction potential (ca. -400 mV). It was proposed that the higher reduction potential of bovine ferredoxin arises from the interaction of His<sup>56</sup> with the iron-sulfur cluster and that a hydrogen bond is formed between the imidazole and a labile sulfide of the

cluster (Lambeth et al., 1982; Usanov et al., 1990). Thus, the characterization of the properties of the histidine residues of vertebrate ferredoxins is of biochemical interest.

Greenfield et al. (1989) carried out the first NMR study of the histidines of a vertebrate ferredoxin. From the pH dependence of the imidazole <sup>1</sup>H<sup>ε1</sup> and <sup>1</sup>H<sup>ε2</sup> signals from bovine ferredoxin, they determined the  $pK_a$  values of the imidazole side chains of two of the three histidines in both the oxidized and reduced states of the protein. They also assigned a peak to <sup>1</sup>H<sup>ε1</sup> of His<sup>56</sup>, but were unable to follow its pH dependence. Subsequently, Miura and Ichikawa (1991a) assigned signals from two of the histidines specifically to His<sup>10</sup> and His<sup>62</sup> by comparing the 1D and 2D <sup>1</sup>H NMR spectra of bovine ferredoxin with the spectra of ovine ferredoxin, which lacks His<sup>10</sup>. However, they proposed a different assignment for His<sup>56</sup> (Miura & Ichikawa, 1991b; Miura et al., 1991). The paramagnetically shifted (hyperfine) signals of several vertebrate ferredoxins (including human and bovine) also have been reported (Skjeldal et al., 1991), but these studies did not reveal any signals that could be assigned to a histidine residue interacting with the iron-sulfur cluster.

We present here a detailed analysis of the <sup>1</sup>H, <sup>13</sup>C, and <sup>15</sup>N NMR spin systems of the three histidines of oxidized and reduced human ferredoxin and an investigation of the pH and temperature dependencies of the <sup>1</sup>H signals. Resonances from His<sup>56</sup> were assigned here by mutagenesis; signals from the other two histidines (His<sup>10</sup> and His<sup>62</sup>) were assigned by analogy to the signals of homologous residues in bovine ferredoxin (Miura & Ichikawa, 1991a). The results indicate that none of these three histidine residues interacts directly with the [2Fe-2S] cluster and that His<sup>56</sup>, proposed to be responsible for the pH dependence of the redox potential in bovine ferredoxin, does not titrate between pH\* 6.0 and 8.6 in either the oxidized or the reduced form of human ferredoxin.

## MATERIALS AND METHODS

**Chemicals and Escherichia coli Strains.** DTT was purchased from Boehringer-Mannheim Biochemicals (Indianapolis, IN) or Sigma (San Diego, CA). <sup>15</sup>NH<sub>4</sub>Cl was purchased from CIL (Cambridge Isotope Laboratories, Woburn, MA). Sodium dithionite (assay >87%) was purchased from Fluka (Fluka Chemical Corp., Ronkonkoma, NY). The 26% labeled [U-<sup>13</sup>C]His was isolated from a protein hydrolyzate of *Anabaena* 7120 (a photosynthetic cyanobacterium) grown on 26% labeled [<sup>13</sup>C]CO<sub>2</sub> as its sole carbon source. *E. coli* strain BL21(DE3)/pLysS was purchased from Novagen (Madison, WI). *E. coli* strain AW608Thr<sup>+</sup>T7/pLysS was prepared by p1 transduction by Dr. Andrew P. Hinck at the University of Wisconsin-Madison.

**Protein and NMR Sample Preparation.** The His<sup>56</sup> to Arg (H56R) and His<sup>56</sup> to Gln (H56Q) mutants of human ferredoxin were prepared and purified at the University of California-Irvine by methods described previously (Coghlan & Vickery, 1991). UV-visible absorption spectra and far-UV CD spectra of H56R and H56Q were indistinguishable from those of wild-type human ferredoxin, and preliminary measurements of electron transfer activity showed both mutants to be active over the pH range 6.4-8.4. At the University of Wisconsin-Madison, human ferredoxin was overexpressed in *E. coli* by using the T7 bacteriophage RNA

polymerase/promoter expression system (Studier & Moffatt, 1986). The cDNA encoding human ferredoxin (Mittal et al., 1988; Coghlan & Vickery, 1989) was cloned into expression vector pET9a to yield a new plasmid HuFd/pET9a. This new plasmid was transformed into *E. coli* strain BL21/pLysS for protein expression.

A test tube with 5 mL of LB medium inoculated from one bacterial colony isolated from an agar plate was incubated in a shaker at 37 °C. After overnight growth, this 5 mL culture was used to inoculate 1 L of LB medium in a 2.8 L Erlenmeyer flask. The culture was incubated in a 37 °C shaker, and 100 mg of IPTG was added to induce protein expression when the OD<sub>600</sub> of the cell culture reached 0.6. After further incubation at 37 °C for about 20 h, the bacteria were harvested by centrifugation and resuspended in 20 mL of Tris buffer (50 mM, pH 7.4).

The cells were lysed by a freeze–thaw cycle followed by sonication. The protein was purified first by *in vitro* reconstitution (Coghlan & Vickery, 1989), and the reconstituted ferredoxin was purified further by using ion-exchange chromatography and gel filtration. Protein fractions with OD<sub>414</sub>/OD<sub>276</sub> > 0.78 were used for further study.

About 20 mg of human ferredoxin was used for each NMR sample, with concentrations around 2 mM. Amicon-stirred cells and YM10 membranes were used to concentrate the protein and to exchange the buffer. Most of the NMR samples were in 50 mM sodium phosphate buffer containing 50 mM NaCl in <sup>2</sup>H<sub>2</sub>O. Protein concentrations were determined by assuming  $E_{414} = 11 \text{ (mM cm)}^{-1}$  (Huang & Kimura, 1973). The pH of samples was adjusted by adding <sup>2</sup>HCl or NaO<sup>2</sup>H.

In order to perform the pH titration study of oxidized human ferredoxin, 15 protein samples in 50 mM Tris-HCl buffer in <sup>2</sup>H<sub>2</sub>O were prepared, each with a protein concentration of ~2 mM. The pH\* value of each sample was adjusted to the desired value by adding 0.5 M <sup>2</sup>HCl or NaO<sup>2</sup>H to the NMR tube. The pH\* values were measured before and after NMR data collection. 1D <sup>1</sup>H NMR spectra were taken on a Bruker AM600 spectrometer with water presaturation.

To reduce human ferredoxin, the protein samples were first deaerated by vacuum; then 2 mg of sodium dithionite was added directly to each sample. The NMR tube was sealed by flame under vacuum. The pH\* values were not measured after the proteins were reduced; the pH\* values indicated for reduced proteins are those measured before the samples were reduced.

**Preparation of Labeled Protein Samples.** Uniformly <sup>15</sup>N-labeled human ferredoxin was prepared as follows. One bacterial colony of *E. coli* strain BL21/pLysS with plasmid HuFd/pET9a was grown in 5 mL of LB medium with 100 mg/L kanamycin and 34 mg/L chloramphenicol for 10 h. This cell culture (100 μL) was used to inoculate 50 mL of labeled M9 medium. Each liter of this medium contained the following: 6 g of Na<sub>2</sub>HPO<sub>4</sub>, 3 g of KH<sub>2</sub>PO<sub>4</sub>, 0.5 g of NaCl, 0.25 g of MgSO<sub>4</sub>·7H<sub>2</sub>O, 0.001 g of thiamine, 5 g of glucose, 1 g of 99.8% <sup>15</sup>N-enriched NH<sub>4</sub>Cl, kanamycin, and chloramphenicol. After overnight incubation in a 37 °C shaker, this 50 mL culture was transferred into a 2.8 L flask containing 950 mL of the same labeled M9 medium. The culture was incubated at 37 °C until the OD<sub>600</sub> reached 0.6. IPTG (100 mg) was added to induce the expression of T7 RNA polymerase. After 16 h, the bacteria were harvested by centrifugation.

In order to selectively label human ferredoxin with [<sup>13</sup>C]-histidine, the plasmid HuFd/pET9a was transformed into a histidine auxotrophic *E. coli* strain, AW608Thr<sup>+</sup>T7/pLysS. An M9 minimal medium containing a mixture of unlabeled L-amino acids was used for bacterial growth. The L-amino acid mixture contained the following (per liter of culture): 0.50 g of alanine, 0.40 g of arginine, 0.40 g of aspartic acid, 0.40 g of asparagine, 0.65 g of glutamine, 0.65 g of glutamic acid, 0.55 g of glycine, 0.23 g of isoleucine, 0.23 g of leucine, 0.42 g of lysine hydrochloride, 0.25 g of methionine, 0.13 g of phenylalanine, 0.10 g of proline, 2.10 g of serine, 0.23 g of threonine, 0.17 g of tyrosine, and 0.23 g of valine. The amino acid mixture was dissolved in 900 mL of H<sub>2</sub>O together with 6 g of Na<sub>2</sub>HPO<sub>4</sub>, 3 g of KH<sub>2</sub>PO<sub>4</sub>, and 1 g of NaCl. After this solution was autoclaved, 100 mL of a separate autoclave-sterilized solution (containing 5 g of glucose and 210 mg of MgSO<sub>4</sub>·7H<sub>2</sub>O) and 5 mL of a filter-sterilized solution (containing 50 mg of L-tryptophan, 50 mg of thiamine, 100 mg of kanamycin, and 34 mg of chloramphenicol) were added. A 5 mL filter-sterilized solution containing 100 mg of 26% uniformly <sup>13</sup>C-labeled histidine was also added to the medium. The bacterial growth procedure was the same as that described earlier for the preparation of <sup>15</sup>N-labeled protein. The labeled human ferredoxins were purified as apoproteins, and the iron–sulfur clusters were inserted *in vitro* as described earlier.

**NMR Spectroscopy.** One- and two-dimensional <sup>1</sup>H NMR spectra were taken on Bruker AM-500 or AM-600 spectrometers at a spectral width of 12 ppm. The sample temperature was 25 °C. For one-dimensional experiments, a normal one-pulse sequence was used with a 90° pulse; a delay of 2 μs followed each data acquisition. The water resonance was suppressed by presaturation for 1.2–1.5 s. Two-dimensional, phase-sensitive, double-quantum-filtered <sup>1</sup>H{<sup>1</sup>H} correlated spectra (DQF-COSY) (Rance et al., 1983) were acquired with the  $D_1-90^\circ-D_0-90^\circ-D_3-90^\circ$ -acq pulse sequence. A total of 4096 data points was collected in  $t_2$  with 512 FIDs in  $t_1$ , and 64 transients were accumulated for each FID. Before Fourier transformation in each dimension, the data were multiplied by a phase-shifted, skewed, sine-bell window function.

<sup>1</sup>H chemical shifts were measured relative to internal DSS (taken as 0 ppm). <sup>13</sup>C chemical shifts were measured relative to external 20 mM [2-<sup>13</sup>C]sodium acetate in 99.8% <sup>2</sup>H<sub>2</sub>O (taken as 24.5 ppm relative to TMS). <sup>15</sup>N chemical shifts were calibrated relative to [<sup>15</sup>N]acetylglutamine (taken as 120 ppm relative to the chemical shift of liquid ammonia).

(1) **<sup>1</sup>H-Detected Heteronuclear Single- and Multiple-Quantum Correlation Spectroscopy (<sup>1</sup>H{<sup>13</sup>C,<sup>15</sup>N}SMQC).** The following pulse sequence was used (Zuiderweg, 1990):

1H: 90°–τ–90°– $t_1/2$ –180°– $t_1/2$ –90°–τ–acq( $t_2$ )  
 X: 90° 90° decouple

The delay time τ was set to be  $(1/2)^{1/2}J_{\text{HX}}$ , i.e., 2.78 ms for the aromatic region of <sup>1</sup>H{<sup>13</sup>C} spectra and 5.56 ms for the <sup>1</sup>H{<sup>15</sup>N} spectra. Only data for the aromatic region were collected. In each case, the carrier frequency was adjusted to be at the center of the region of interest. For each  $t_1$ , 2048 data points were collected in  $t_2$ . Prior to Fourier transformation in each dimension, a sine-squared window function with a 90° phase shift was applied.

(2) **<sup>1</sup>H-Detected Heteronuclear Multiple-Bond <sup>1</sup>H–<sup>13</sup>C and <sup>1</sup>H–<sup>15</sup>N Correlation Spectroscopy (<sup>1</sup>H{<sup>13</sup>C,<sup>15</sup>N}MBC).** This

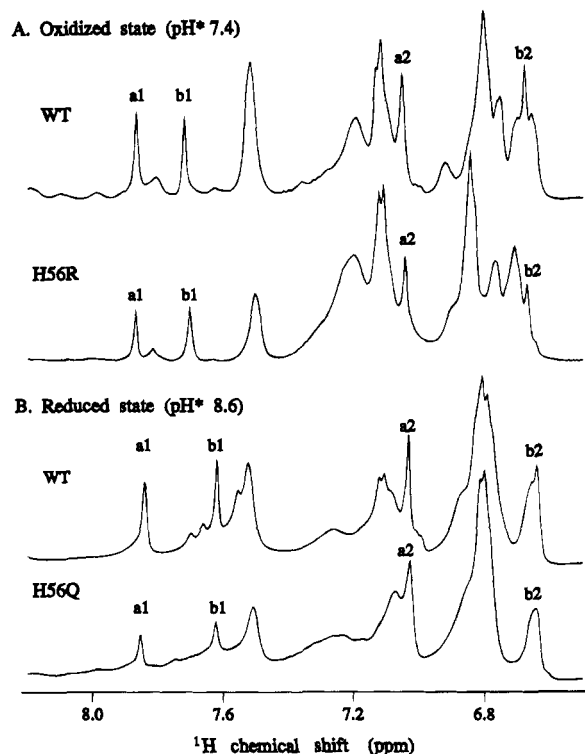


FIGURE 2: (A) Aromatic region of one-dimensional  $^1\text{H}$  NMR spectra (500 MHz) of wild-type human ferredoxin and mutant H56R at pH\* 7.4 in the oxidized state. (B) Aromatic region of one-dimensional  $^1\text{H}$  NMR spectra (500 MHz) of wild-type human ferredoxin and mutant H56Q at pH\* 8.6 in the reduced state. The sample temperature was 25 °C. Peaks a1 and b1 are assigned to the  $\epsilon 1$  protons and peaks a2 and b2 to the  $\delta 2$  protons of two of the three histidines in wild-type human ferredoxin. (pH\* measurements were taken before the protein was reduced.)

experiment was performed according to the following pulse sequence (Bax & Summers, 1986; Summers et al., 1986):

$$\begin{array}{l} ^1\text{H: } 90^\circ - \tau_1 - \tau_2 - t_1/2 - 180^\circ - t_1/2 - \text{acq}(t_2) \\ \text{X: } 90^\circ - \tau_2 - 90^\circ \quad \quad \quad 90^\circ \text{ decouple} \end{array}$$

The delay time  $\tau_1$  served to eliminate single-bond correlations ( $\tau_1 = 2.78$  ms for  $^1\text{H}\{^{13}\text{C}\}$  experiments, and  $\tau_1 = 5.56$  ms for  $^1\text{H}\{^{15}\text{N}\}$  spectra), while  $\tau_2$  was set to optimize two- and three-bond coupling ( $\tau_2 = 60$  ms). The data set consisted of 512  $t_1$  increments of 2048 data points each. A window function of sine squared with a  $90^\circ$  phase shift was applied to both  $t_1$  and  $t_2$  dimensions. Following Fourier transformation, spectra were phased in the  $t_1$  dimension and magnitude calculated in the  $t_2$  dimension.

## RESULTS AND DISCUSSION

**Homonuclear  $^1\text{H}$  NMR Spectroscopy.** One-dimensional  $^1\text{H}$  NMR spectra of oxidized (pH\* 7.4) and reduced (pH\* 8.6) wild-type human ferredoxin and its mutants, H56R and H56Q, are shown in Figure 2. Four sharp peaks (a1, b1, a2, and b2), present in the spectra of both oxidized and reduced wild-type human ferredoxin, exhibit pH-dependent chemical shifts. In the initial NMR study of bovine ferredoxin, sharp peaks in corresponding positions were attributed to His<sup>10</sup> and His<sup>62</sup> (Greenfield et al., 1989), since it was assumed that the signals from His<sup>56</sup> would be broadened by their proximity to the [2Fe-2S] center. As a test of this assignment, we mutated histidine 56 of human

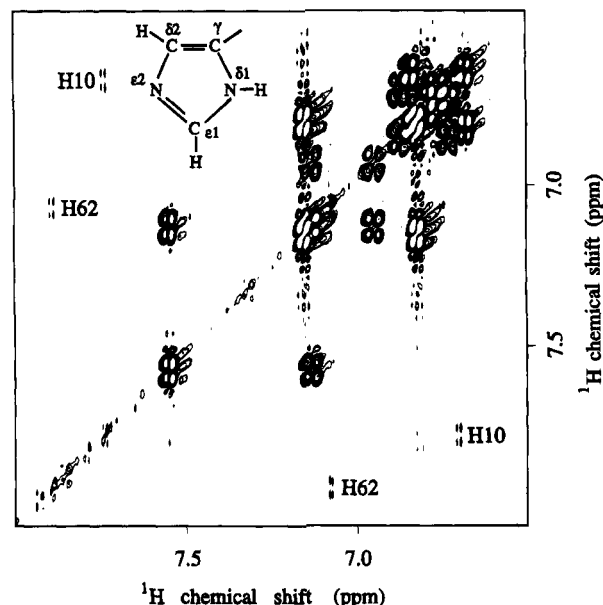


FIGURE 3: Aromatic region of the two-dimensional  $^1\text{H}$  NMR DQF-COSY spectrum of oxidized human ferredoxin at 500 MHz in  $^2\text{H}_2\text{O}$  at 25 °C and pH\* 7.4. The spectrum was recorded with a 6024 Hz spectral width; 64 scans were accumulated for each  $t_1$  value, and 512 increments were collected. Four cross peaks arising from imidazole group  $^1\text{H}^{\epsilon 1}$ – $^1\text{H}^{\delta 2}$  couplings are indicated. The inset shows the chemical structure of the imidazole side chain with the atom-labeling scheme employed here.

ferredoxin to arginine and glutamine. As shown in Figure 2, all four histidine peaks (a1, b1, a2, and b2) are retained in spectra of the mutants in both oxidation states; thus these peaks arise from His<sup>10</sup> and His<sup>62</sup> as suggested for bovine ferredoxin (Greenfield et al., 1989; Miura & Ichikawa, 1991a), and the resonances from His<sup>56</sup> must lie elsewhere.

As noted earlier, Miura and Ichikawa (1991a) used 1D and 2D  $^1\text{H}$  NMR to study bovine and ovine ferredoxins. By comparing COSY data from the two proteins, they were able to assign peaks individually to the imidazole rings of His<sup>10</sup> and His<sup>62</sup>. The two-dimensional DQF-COSY spectrum of oxidized human ferredoxin (Figure 4) was collected in 50 mM sodium phosphate/50 mM sodium chloride buffer in 99.9%  $^2\text{H}_2\text{O}$  with pH\* 7.4. The cross peaks from long range couplings between the  $^1\text{H}^{\epsilon 1}$  and  $^1\text{H}^{\delta 2}$  of two histidines can be easily recognized. The close correspondence between this spectrum and those reported by Miura and Ichikawa (1991a) allows us to assign peaks a1 and a2, respectively, to the  $\epsilon 1$  and  $\delta 2$  protons of His<sup>62</sup> and peaks b1 and b2 to the  $\epsilon 1$  and  $\delta 2$  protons of His<sup>10</sup>. The nomenclature for each atom of the histidine imidazole side chain is shown in Figure 3.

**Effects of pH on the Histidine  $^1\text{H}$  NMR Signals.** The  $\text{pK}_a$  values for His<sup>10</sup> and His<sup>62</sup> of oxidized human ferredoxin were determined from the pH dependencies of their chemical shifts. The pH titration study covered the range between pH\* 5.85 and 10.5. The protein began to precipitate out of solution at pH\* values below 5.8. The pH titration curves were fitted to a modified Henderson–Hasselbalch equation,

$$\delta_{\text{obs}} = \frac{\delta_{\text{AH}^+} + \delta_{\text{A}} 10^{(\text{pH} - \text{pK}_a)}}{1 + 10^{(\text{pH} - \text{pK}_a)}} \quad (1)$$

or to a Hill plot equation,

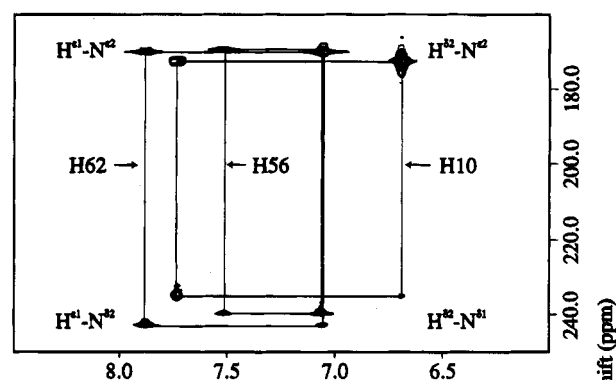
$$\frac{\delta_A - \delta_{\text{obs}}}{\delta_{\text{obs}} - \delta_{\text{AH}^+}} = e^{n(\text{pH} - \text{pK}_a)} \quad (2)$$

where  $\delta_{\text{obs}}$  is the chemical shift observed at each pH value,  $\delta_{\text{AH}^+}$  and  $\delta_A$  are the chemical shifts for the protonated and deprotonated histidines, respectively, and  $n$  is the Hill coefficient. The fitting parameters and results are given in Table 1. Since signal overlaps made the pH dependencies of the  $^1\text{H}^{\delta 2}$  resonances difficult to follow, the titration results are solely from the histidine  $^1\text{H}^{\epsilon 1}$  data. The  $\text{pK}_a$  for His<sup>10</sup> is 6.45 and that of His<sup>62</sup> is 5.78; both values are lower than the histidine  $\text{pK}_a$  value (6.9) reported from the study of a model peptide (Markley, 1975). They are also lower than the  $\text{pK}_a$  values reported for bovine ferredoxin: 6.61 and 6.12 in Greenfield et al. (1989); 6.6 and 6.0 in Miura et al. (1991).

**Multinuclear NMR Studies.** In order to assign the imidazole proton and nitrogen spin systems of all three histidines (Table 2),  $^1\text{H}\{^{15}\text{N}\}$ MBC spectra were taken of both oxidized and reduced 99% uniformly  $^{15}\text{N}$ -labeled human ferredoxin at pH\* 7.4. In the  $^1\text{H}\{^{15}\text{N}\}$ MBC spectra, the  $^1\text{H}^{\epsilon 1}$ – $^{15}\text{N}^{\epsilon 2}$ ,  $^1\text{H}^{\epsilon 1}$ – $^{15}\text{N}^{\delta 1}$ ,  $^1\text{H}^{\delta 2}$ – $^{15}\text{N}^{\epsilon 2}$ , and  $^1\text{H}^{\delta 2}$ – $^{15}\text{N}^{\delta 1}$  crosspeaks from imidazole form a rectangle (Oh et al., 1990). Connectivities corresponding to all three histidines were present in the spectrum of oxidized human ferredoxin (Figure 4A). Two of these corresponded to the His<sup>10</sup> and His<sup>62</sup> resonances assigned earlier (Figures 2 and 3). The remaining spin system was assigned to His<sup>56</sup>. The  $^1\text{H}^1$  peak of His<sup>56</sup> (7.50 ppm) is not resolved from the broad phenylalanine peak in the 1D spectrum, making it difficult to observe (Figure 2). The  $^1\text{H}^{\delta 2}$  peak of His<sup>56</sup> (7.05 ppm) is almost at the same chemical shift as the  $^1\text{H}^{\delta 2}$  peak of His<sup>62</sup> at this pH\*.

Two complete imidazole spin systems were observed in the  $^1\text{H}\{^{15}\text{N}\}$ MBC spectrum of reduced human ferredoxin: those of His<sup>10</sup> and His<sup>62</sup> (Figure 4B). Only half of the expected cross peaks were seen for His<sup>56</sup>: those from  $^1\text{H}^{\epsilon 1}$ – $^{15}\text{N}^{\epsilon 2}$  and  $^1\text{H}^{\epsilon 1}$ – $^{15}\text{N}^{\delta 1}$  couplings, which determined the

#### A. Oxidized human ferredoxin



#### B. Reduced human ferredoxin

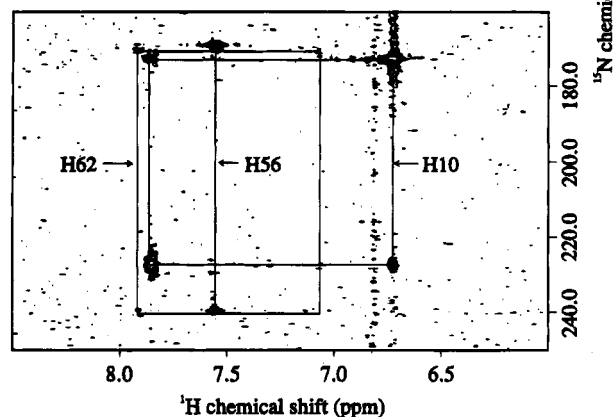


FIGURE 4: Two-dimensional 600 MHz  $^1\text{H}\{^{15}\text{N}\}$ MBC spectrum of uniformly  $^{15}\text{N}$ -labeled human ferredoxin in  $\text{D}_2\text{O}$ . The data were recorded selectively for the His region in the  $^{15}\text{N}$  dimension, with 512 increments and 128 scans for each  $t_1$  value. The sweep width for the  $^{15}\text{N}$  dimension was 117.5 ppm. Rectangular connectivities are shown that link cross peaks from multiple-bond  $^1\text{H}$ – $^{15}\text{N}$  couplings in the imidazole ring of each of the three histidines. (A) Oxidized state at pH\* 7.4. (B) Reduced state at pH\* 7.4 (the pH\* measurement before the protein was reduced by added dithionite).

Table 1: Comparison of the Histidine pH Titration Parameters of Oxidized Human and Bovine Ferredoxins<sup>a</sup>

ferredoxin	histidine	proton	Henderson–Hasselbalch equation				Hill plot	
			$\text{pK}_a$	$\delta_{\text{AH}^+}$	$\delta_A$	$\Delta\delta_{\text{AH}^+ - A}$	$\text{pK}_a$	Hill coefficient
human	His <sup>10</sup>	$\text{H}^{\epsilon 1}$	6.45	8.88	7.59	1.29	6.46	0.99
	His <sup>62</sup>	$\text{H}^{\epsilon 1}$	5.78	9.19	7.83	1.26	5.78	1.01
bovine <sup>b</sup>	His <sup>10</sup>	$\text{H}^{\epsilon 1}$	6.55	8.65	7.59	1.06		
	His <sup>62</sup>	$\text{H}^{\epsilon 1}$	6.14	8.45	7.83	0.62		

<sup>a</sup>The chemical shifts of histidines in their protonated ( $\delta_{\text{AH}^+}$ ) and deprotonated ( $\delta_A$ ) states and  $\Delta\delta_{\text{AH}^+ - A}$  are the results of nonlinear least-squares fitting of the experimental data to a modified Henderson–Hasselbalch equation. The  $\text{pK}_a$  values were calculated without and with a variable Hill coefficient. No attempt was made to correct the  $\text{pK}_a$  and pH values for deuterium isotope effects. <sup>b</sup>The pH titration data for bovine ferredoxin are from Greenfield et al. (1989), with assignments from Miura and Ichikawa (1991a).

Table 2: NMR Chemical Shifts of the Histidine Imidazoles of Oxidized and Reduced Human Ferredoxin at 25 °C<sup>a</sup>

residue	chemical shifts (ppm) in oxidized state						
	$\text{H}^{\epsilon 1}$	$\text{H}^{\delta 2}$	$\text{N}^{\epsilon 2}$	$\text{N}^{\delta 1}$	$\text{C}^{\epsilon 1}$	$\text{C}^{\delta 2}$	$\text{C}^{\gamma}$
His <sup>10</sup>	7.72 (7.70) <sup>b</sup>	6.67 (6.67) <sup>b</sup>	172.7	235.0	136.6	118.0	133.6
His <sup>56</sup>	7.50 (7.52) <sup>c</sup>	7.05	169.6	240.0	135.7	124.2	
His <sup>62</sup>	7.87 (7.87) <sup>b</sup>	7.05 (7.04) <sup>b</sup>	170.1	242.9	137.4	115.9	134.3
residue	chemical shifts (ppm) in reduced state						
	$\text{H}^{\epsilon 1}$	$\text{H}^{\delta 2}$	$\text{N}^{\epsilon 2}$	$\text{N}^{\delta 1}$	$\text{C}^{\epsilon 1}$	$\text{C}^{\delta 2}$	$\text{C}^{\gamma}$
His <sup>10</sup>	7.78 (7.76) <sup>c</sup>	6.71 (6.71) <sup>c</sup>	172.9	227.5	136.5	118.3	132.7
His <sup>56</sup>	7.55/7.72 <sup>d,e</sup>	7.14/6.80 <sup>d</sup>	169.2	239.8	135.8	124.9/116.2 <sup>d</sup>	
His <sup>62</sup>	7.89 (7.91) <sup>c</sup>	7.07 (7.06) <sup>c</sup>	170.6	240.2	137.3	116.3	

<sup>a</sup>The pH\* of the oxidized protein was 7.4; pH\* values were not measured after reducing the protein. The numbers indicated in parentheses are the chemical shifts of corresponding protons in bovine ferredoxin at comparable pH\*. <sup>b</sup>Bovine ferredoxin chemical shifts are from Greenfield et al. (1989). <sup>c</sup>Bovine ferredoxin chemical shifts are from Miura and Ichikawa (1991a). <sup>d</sup>Peak doubling caused by apparent conformational heterogeneity. <sup>e</sup>A single peak at 7.83 ppm was assigned to the  $^1\text{H}^{\epsilon 1}$  of His<sup>56</sup> in reduced bovine ferredoxin (Miura & Ichikawa, 1991b).

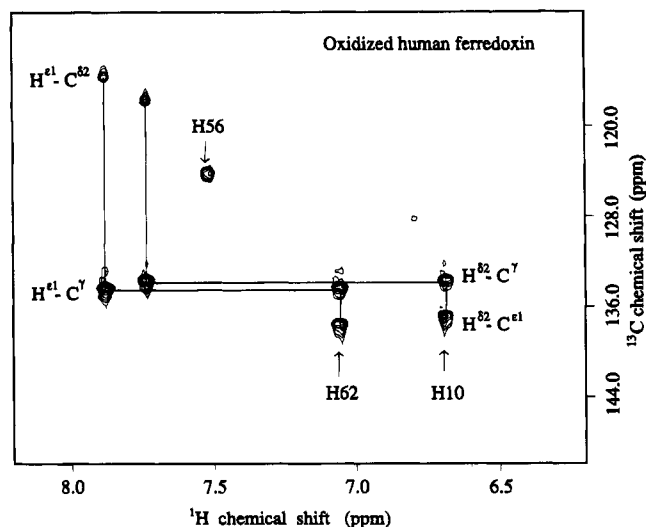


FIGURE 5:  $^1\text{H}\{^{13}\text{C}\}$ MBC spectrum (600 MHz  $^1\text{H}$ , 150.924 MHz  $^{13}\text{C}$ ) of 26%  $^{13}\text{C}$ -His-labeled human ferredoxin in the oxidized state at pH\* 7.4 in  $\text{D}_2\text{O}$ . The data were collected in 512 blocks, with 64 average FIDs per  $t_1$  value and with 120 ppm for the  $^{13}\text{C}$  spectral width. His<sup>10</sup> and His<sup>62</sup> showed all four of the expected multiple-bond  $^1\text{H}$ – $^{13}\text{C}$  coupling cross peaks. His<sup>56</sup> showed only one such cross peak.

chemical shift for the  $\epsilon 1$  proton of His<sup>56</sup> at 7.55 ppm. According to this chemical shift, the small peak at 7.55 ppm on the shoulder of the larger peak at 7.50 ppm in the 1D  $^1\text{H}$  NMR spectra of reduced protein (Figure 2) was assigned to the  $^1\text{H}^{\epsilon 1}$  of His<sup>56</sup>. The preceding assignments were confirmed by examining the 1D  $^1\text{H}$  NMR spectrum of the same sample without  $^{15}\text{N}$  decoupling, which showed the splitting of the signals assigned to the  $^1\text{H}^{\epsilon 1}$  protons of the three histidines due to coupling to  $^{15}\text{N}^2$  and  $^{15}\text{N}^1$  of the imidazole ring (spectrum not shown).

$^1\text{H}\{^{13}\text{C}\}$ SMQC and  $^1\text{H}\{^{13}\text{C}\}$ MBC data from 26% labeled  $[\text{U-}^{13}\text{C}]$ histidine human ferredoxin in the oxidized and reduced states at pH\* 7.4 were used to assign the carbon resonances of the three histidines (Table 2). All six of the peaks expected in the  $^1\text{H}\{^{13}\text{C}\}$ SMQC spectrum of the oxidized protein (spectrum not shown) were resolved and assigned to  $^1\text{H}$ – $^{13}\text{C}$  single-bond couplings. The  $^1\text{H}\{^{13}\text{C}\}$ -MBC spectrum of oxidized human ferredoxin (Figure 5) contained the full set of cross peaks expected from multiple-bond couplings ( $^1\text{H}^{\epsilon 1}$ – $^{13}\text{C}^{\delta 2}$ ,  $^1\text{H}^{\epsilon 1}$ – $^{13}\text{C}^{\gamma}$ ,  $^1\text{H}^{\delta 2}$ – $^{13}\text{C}^{\gamma}$ ,  $^1\text{H}^{\delta 2}$ – $^{13}\text{C}^{\epsilon 1}$ ) for His<sup>10</sup> and His<sup>62</sup>, but only one cross peak ( $^1\text{H}^{\epsilon 1}$ – $^{13}\text{C}^{\delta 2}$ ) from His<sup>56</sup>.

The  $^1\text{H}\{^{13}\text{C}\}$ SMQC spectrum of reduced human ferredoxin (Figure 6) showed eight peaks from histidine side-chain  $^1\text{H}$ – $^{13}\text{C}$  single-bond couplings. Four of these peaks were assigned to His<sup>10</sup> and His<sup>62</sup> by comparing this spectrum with the  $^1\text{H}\{^{13}\text{C}\}$ SMQC and  $^1\text{H}\{^{13}\text{C}\}$ MBC data (Table 2). The  $^{13}\text{C}$  chemical shifts of the histidines are little changed upon reduction. Interestingly, doubling of some of the signals assigned to His<sup>56</sup> provides clear evidence for the existence of two conformational states in the reduced form of the protein. As will be discussed later, the  $^1\text{H}^{\epsilon 1}$ ,  $^1\text{H}^{\delta 2}$ , and  $^{13}\text{C}^{\delta 2}$  chemical shifts of His<sup>56</sup> differ in the two forms.

**Temperature Dependence of Spectra.** Figure 7 shows the temperature dependence of the  $\epsilon 1$  protons of the three histidines. The thermal independence of the chemical shifts of His<sup>56</sup> indicates that the side chain of this residue does not interact directly with the iron–sulfur cluster. The other two

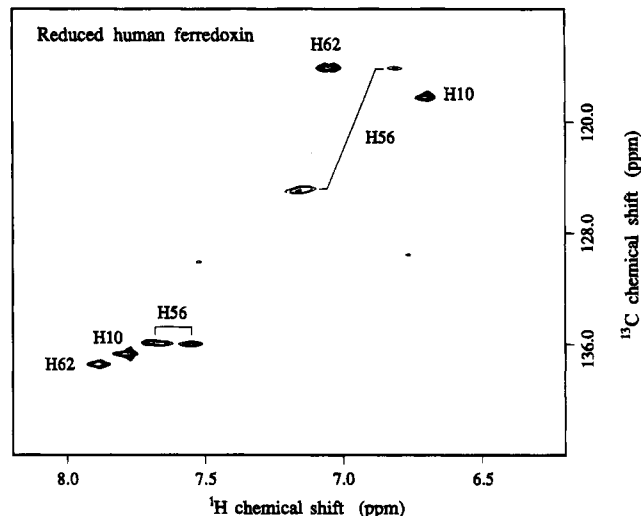


FIGURE 6: Two-dimensional 600-MHz  $^1\text{H}\{^{13}\text{C}\}$ SMQC spectrum of 26%  $^{13}\text{C}$ -His-labeled human ferredoxin in the reduced state at pH\* 7.4 in  $\text{D}_2\text{O}$ : 512 increments were acquired with 64 averaged FIDs per  $t_1$  value. All six of the cross peaks indicated are from one-bond  $^1\text{H}$ – $^{13}\text{C}$  couplings in the imidazole rings.

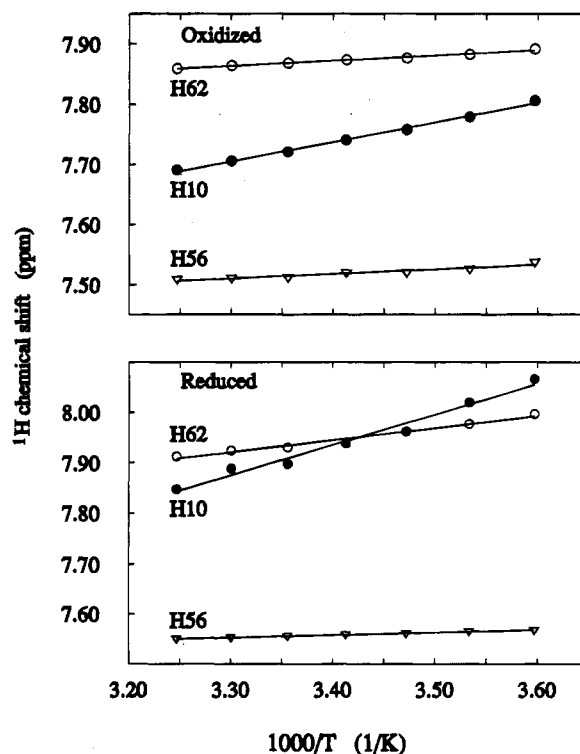


FIGURE 7: Temperature dependence of the histidine imidazole ring  $\epsilon 1$  protons: His<sup>10</sup>, ●; His<sup>56</sup>, ▽; His<sup>62</sup>, ○. Upper panel, oxidized ferredoxin; lower panel, reduced ferredoxin.

histidines show small temperature effects (larger for His<sup>10</sup> than for His<sup>62</sup>); these are too small to be hyperfine effects and probably arise from a linear increase in the  $\text{pK}_a$  values of these residues with  $1/T$ , as was observed for the His<sup>16</sup> of *Anabaena variabilis* ferredoxin II (Chan & Markley, 1983).

**Environment and Properties of Histidine 56.** In order to study the pH dependence of His<sup>56</sup> and the conformational heterogeneity in greater detail, 1D  $^{13}\text{C}$ -edited  $^1\text{H}$  NMR data were collected for oxidized and reduced 26% uniformly  $^{13}\text{C}$ -His-labeled human ferredoxin at pH\* 6.0, 7.4, and 8.6. Figure 8A shows the spectra of oxidized human ferredoxin at these three pH\* values. It is evident that the chemical shifts of the  $^1\text{H}^{\epsilon 1}$  ( $\epsilon 1$ , 7.50) and  $^1\text{H}^{\delta 2}$  ( $\epsilon 2$ , 7.05) protons of

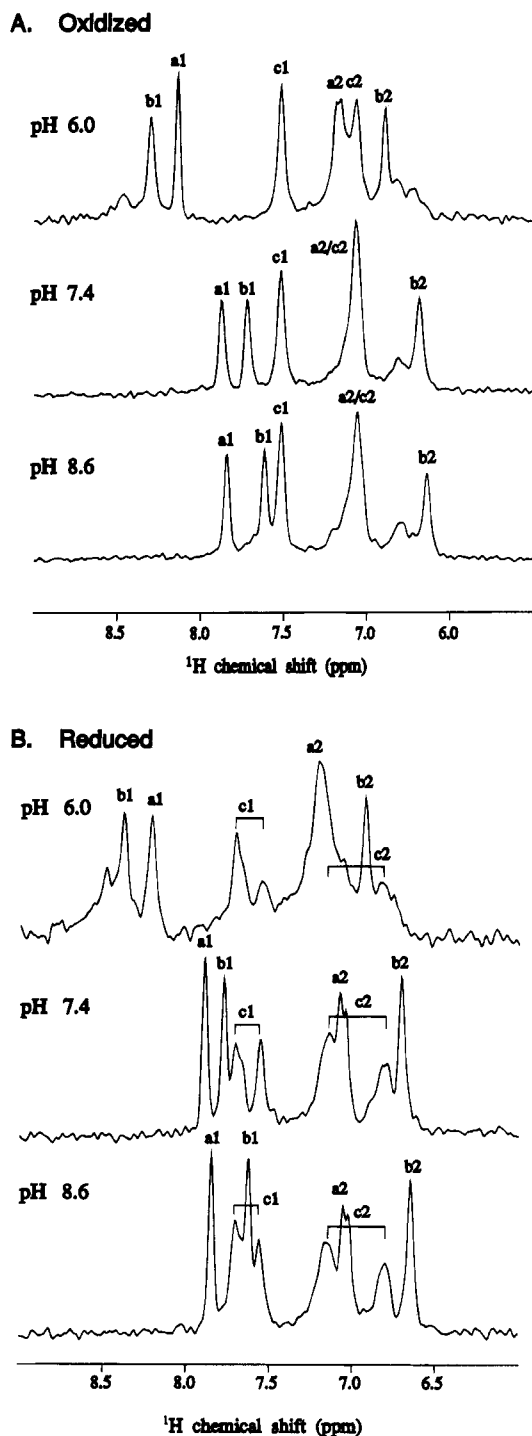


FIGURE 8: Aromatic region of the one-dimensional,  $^{13}\text{C}$ -edited  $^1\text{H}$  NMR spectrum of 26%  $^{13}\text{C}$ -labeled ferredoxin at 25 °C and at the three pH\* values indicated in the figure: (A) oxidized state; (B) reduced state.

His<sup>56</sup> have little or no pH dependence in this pH range (pH\* 6.0–8.6). The  $^{13}\text{C}$ -edited  $^1\text{H}$  NMR spectra of reduced 26% uniformly  $^{13}\text{C}$ -labeled human ferredoxin (Figure 8B) confirm the existence of two distinct conformations in the region of His<sup>56</sup>: doubled peaks at chemical shifts 7.55 and 7.72 ppm are assigned to His<sup>56</sup>  $^1\text{H}^{\epsilon 1}$ , and doubled peaks at 7.14 and 6.80 ppm are assigned to His<sup>56</sup>  $^1\text{H}^{\delta 2}$ . The relative intensities of the peaks give a population ratio for the two states of about 3:1. Since the effect is slow on the NMR time scale, one can place a lower limit on the lifetimes of the two states (about 10 ms) from the smallest resolved splitting. Additional studies will be required in order to

determine the structural origin of the two states.

As observed for the oxidized protein, the signals originating from His<sup>56</sup> do not titrate within the pH range studied (pH\* 6.0–8.0). The  $^{15}\text{N}$  NMR chemical shifts of His<sup>56</sup> clearly indicate (Blomberg et al., 1977) that the residue is deprotonated in this range. Thus, its  $\text{pK}_a$  value must be below 5. These results are consistent with those of Miura et al. (1991), which showed that His<sup>56</sup> of oxidized bovine ferredoxin does not exhibit a normal histidine titration curve. They attributed this to an interaction between His<sup>56</sup> and Ser<sup>88</sup>.

## SUMMARY

Histidine 56, which is adjacent to one of the iron–sulfur cluster ligand cysteines (Cys<sup>55</sup>) and is conserved in all vertebrate ferredoxins (Figure 1), is the most interesting of the three histidines of human ferredoxin. Previous studies suggested that His<sup>56</sup> plays an important role in binding with ferredoxin reductase and cytochrome P450<sub>scc</sub> (Miura & Ichikawa, 1991b; Miura et al., 1991). It also was suggested that His<sup>56</sup> is responsible for the pH dependence of the reduction potential of the iron–sulfur cluster (Lambeth et al., 1982; Greenfield et al., 1989).

The peak that Greenfield et al. (1989) assigned to the  $^1\text{H}^{\epsilon 1}$  of His<sup>56</sup> of oxidized bovine ferredoxin corresponds to the small peak near 7.80 ppm between the two  $^1\text{H}^{\epsilon 1}$  peaks of His<sup>10</sup> and His<sup>62</sup> in the 1D  $^1\text{H}$  NMR spectrum of human ferredoxin (Figure 2). In subsequent studies, Ichikawa and co-workers assigned a peak at 7.52 ppm to  $^1\text{H}^{\epsilon 1}$  and one at 7.05 ppm to  $^1\text{H}^{\delta 2}$  of His<sup>56</sup>; these assignments were supported by data from the chemical modification of the histidine with DEP (Miura & Ichikawa, 1991b; Miura et al., 1991). The latter assignments are consistent with the present results with human ferredoxin.<sup>2</sup> In the present study, spectral overlaps in the spectrum of human ferredoxin necessitated the use of  $^{15}\text{N}$  and  $^{13}\text{C}$  labeling and multinuclear NMR methods in order to identify the His<sup>56</sup> spin system unambiguously; these provided complete side-chain  $^1\text{H}$ ,  $^{13}\text{C}$ , and  $^{15}\text{N}$  assignments.

In human ferredoxin, His<sup>10</sup> and His<sup>62</sup> have  $\text{pK}_a$  values of 6.46 and 5.78, respectively (Table 2), and His<sup>56</sup> does not titrate between pH 6.0 and 8.6. The pH independence of its chemical shifts suggests either that the side chain of His<sup>56</sup> forms a strong hydrogen bond or that this residue is in a solvent inaccessible environment. Its  $^{15}\text{N}^{\epsilon 2}$  chemical shift (Table 2) indicates that the imidazole side chain of His<sup>56</sup> is deprotonated in both the oxidized and reduced states. From its abnormal  $\text{pK}_a$  values in both oxidation states, we can conclude that His<sup>56</sup> is not responsible for the pH dependence of the reduction potential. Moreover, the lack of hyperfine interactions with the cluster, as evidenced by the temperature independence of its chemical shifts, indicates that His<sup>56</sup> does not interact directly with the iron–sulfur cluster. Instead, it appears to point away from the cluster and to form an interaction that greatly lowers its  $\text{pK}_a$  value. This interaction may be with Ser<sup>88</sup>, as suggested by Miura et al. (1991) for bovine ferredoxin, since Ser<sup>88</sup> is conserved in human ferredoxin and in all other vertebrate ferredoxins. If the pH dependence of the reduction potential of human ferredoxin is similar to that reported for bovine ferredoxin (pH<sub>mid</sub> ~ 7.2; Cooper et al., 1973), these results rule out the participation of any histidine residues.

<sup>2</sup> In similar studies, Wray and co-workers (1994) used site-directed mutagenesis to confirm this assignment (Miura et al., 1991) of the imidazole ring proton signals from His<sup>56</sup> in oxidized bovine ferredoxin.

Multinuclear NMR data presented here for reduced human ferredoxin reveal doubled peaks for His<sup>56</sup>, which appear to arise from local conformational heterogeneity. Since spectra of the oxidized protein do not show similar doubling, the conformational heterogeneity probably is induced when the protein is reduced. The absence of splitting in NMR signals from the other two histidines suggests that the heterogeneity is localized. The two states have lifetimes in excess of 10 ms and are present at a ratio of about 3:1.

## ACKNOWLEDGMENT

We thank Dr. W. Milo Westler and Dr. Jingfeng Wang for assistance and helpful discussions and Dr. Andrew P. Hinck for kindly providing the histidine auxotrophic *E. coli* strain.

## REFERENCES

- Bax, A., & Summers, M. F. (1986) *J. Am. Chem. Soc.* 108, 2093–2094.
- Blomberg, F., Maurer, W., & Rüterjans, H. (1977) *J. Am. Chem. Soc.* 99, 8149–8159.
- Chae, Y. K., Xia, B., Cheng, H., Oh, B.-H., Skjeldal, L., Westler, W. M., & Markley, J. L. (1994) NATO Advanced Research Workshop on Nuclear Magnetic Resonance of Paramagnetic Macromolecules, Sintra, Portugal, June 4–8, 1994, Abstr. pp 18–19.
- Chan, T.-M., & Markley, J. L. (1983) *Biochemistry* 22, 5982–5987.
- Cheng, H., Xia, B., Reed, G. H., & Markley, J. L. (1994) *Biochemistry* 33, 3155–3164.
- Coghlan, V. M., & Vickery, L. E. (1989) *Proc. Natl. Acad. Sci. U.S.A.* 86, 835–839.
- Coghlan, V. M., & Vickery, L. E. (1991) *J. Biol. Chem.* 266, 18606–18612.
- Cooper, D. Y., Schleyer, H., Levin, S. S., & Rosenthal, O. (1973) *Ann. N.Y. Acad. Sci.* 212, 227–247.
- Cupp, J. R., & Vickery, L. E. (1988) *J. Biol. Chem.* 263, 17418–17421.
- Greenfield, N. J., Wu, X., & Jordan, F. (1989) *Biochim. Biophys. Acta* 995, 246–254.
- Huang, J. J., & Kimura, T. (1973) *Biochemistry* 12, 406–409.
- Hurley, J. K., Cheng, H., Xia, B., Markley, J. L., Medina, M., Carlos, G.-M., & Tollin, G. (1993) *J. Am. Chem. Soc.* 115, 11698–11701.
- Kagimoto, K., McCarthy, J. L., Waterman, M. R., & Kagimoto, M. (1988) *Biochem. Biophys. Res. Commun.* 155, 379–383.
- Lambeth, J. D., & Kamin, H. (1979) *J. Biol. Chem.* 254, 2766–2774.
- Lambeth, J. D., Saybert, D. W., Lancaster, J. R., Jr., Salerno, J. C., & Kamin, H. (1982) *Mol. Cell. Biochem.* 45, 13–31.
- Markley, J. L. (1975) *Acc. Chem. Res.* 8, 70–80.
- Mason, J. I., & Boyd, G. S. (1971) *Eur. J. Biochem.* 21, 308–321.
- Matsuo, Y., Tsujita, M., Mizoguchi, K., & Ichikawa, Y. (1992) *FEBS Lett.* 301, 132–136.
- Mellon, S. H., Kushner, J. A., & Vaisse, C. (1991) *DNA Cell Biol.* 10, 339–347.
- Mittal, S., Zhu, Y., & Vickery, L. E. (1988) *Arch. Biochem. Biophys.* 264, 383–391.
- Miura, S., & Ichikawa, Y. (1991a) *Eur. J. Biochem.* 197, 747–757.
- Miura, S., & Ichikawa, Y. (1991b) *J. Biol. Chem.* 266, 6252–6258.
- Miura, S., Tamita, S., & Ichikawa, Y. (1991) *J. Biol. Chem.* 266, 19212–19216.
- Oh, B.-H., Mooberry, E. S., & Markley, J. L. (1990) *Biochemistry* 29, 4004–4011.
- Okamura, T., John, M. E., Zuber, M. X., Simpson, E. R., & Waterman, M. R. (1985) *Proc. Natl. Acad. Sci. U.S.A.* 81, 5705–5709.
- Rance, M., Sørensen, O. W., Bodenhausen, G., Wagner, G., Ernst, R. R., & Wüthrich, K. (1983) *Biochem. Biophys. Res. Commun.* 117, 497–485.
- Simpson, E. R., & Miller, D. A. (1978) *Arch. Biochem. Biophys.* 190, 800–808.
- Skjeldal, L., Markley, J. L., Coghlan, V. M., & Vickery, L. E. (1991) *Biochemistry* 30, 9078–9083.
- Smith, E. T., Tomich, J. M., Iwamoto, T., Richards, J. H., Mao, Y., & Feinberg, B. A. (1991) *Biochemistry* 30, 11669–11676.
- Studier, F. W., & Moffatt, B. A. (1986) *J. Mol. Biol.* 189, 113–130.
- Summers, M. F., Marzilli, L. G., & Bax, A. (1986) *J. Am. Chem. Soc.* 108, 4285–4294.
- Tanaka, M., Haniu, M., Yasunobu, K. T., & Kimura, T. (1973) *J. Biol. Chem.* 248, 1141–1157.
- Usanov, S. A., Chashchin, V. L., & Akhrem, A. A. (1990) *Frontiers in Biotransformation* 3, 1–57.
- Wray, V., Beckert, V., & Bernhardt, R., (1994) NATO Advanced Research Workshop on Nuclear Magnetic Resonance of Paramagnetic Macromolecules, Sintra, Portugal, June 4–8, 1994, Abstr. p 75.
- Zuiderweg, E. R. P. (1990) *J. Magn. Reson.* 86, 346–357.